

MUSE: MULTI-MODAL TARGET SPEAKER EXTRACTION WITH VISUAL CUES

Zexu Pan^{1,2}, Ruijie Tao³, Chenglin Xu³, Haizhou Li^{1,3,4} *

¹Institute of Data Science, NUS, Singapore

²Graduate School for Integrative Sciences and Engineering, NUS, Singapore

³Department of Electrical and Computer Engineering, National University of Singapore (NUS), Singapore

⁴Machine Listening Lab, University of Bremen, Germany

ABSTRACT

Speaker extraction algorithm relies on the speech sample from the target speaker as the reference point to focus its attention. Such a reference speech is typically pre-recorded. On the other hand, the temporal synchronization between speech and lip movement also serves as an informative cue. Motivated by this idea, we study a novel technique to use speech-lip visual cues to extract reference target speech directly from mixture speech during inference time, without the need of pre-recorded reference speech. We propose a multi-modal speaker extraction network, named MuSE, that is conditioned only on a lip image sequence. MuSE not only outperforms other competitive baselines in terms of SI-SDR and PESQ, but also shows superior robustness in cross-domain evaluations.

Index Terms— Multi-modal, target speaker extraction, time domain, robustness

1. INTRODUCTION

Speech separation seeks to separate speakers' voices from a multi-talk acoustic environment, also known as the cocktail party problem [1]. This is a non-trivial task for machines but useful for downstream applications such as speaker verification and speech recognition. Recent advances include computational auditory scene analysis [2], non-negative matrix factorization [3], Deep clustering [4], ConvTasnet [5], and cPIT [6]. However, the formulation of speech separation usually requires the number of speakers to be known in advance, that is not practical in real-world applications.

Humans have the ability to focus the auditory attention to one of the sound sources in a complex cocktail party [7]. Speaker extraction is the technique to emulate such human

ability. It generally requires an auxiliary reference that identifies the target speaker. The reference speech can be considered as an attractor for selective auditory attention. It is usually encoded in an utterance-level speaker embedding as speaker's voice signature [7–9]. One example is VoiceFilter that estimates a speaker-conditioned spectrogram mask for target speaker extraction [8]; SpEx/SpEx+ is another successful implementation that trains speaker embedding network jointly with speaker extraction network [7, 10].

Visual cues also provide informative reference points for target speakers, such as the face or lip image sequences, where phonetic or prosodic content coincides with muscle movement [11–13]. For example, Ephrat et al. uses synchronized face embeddings for speaker extraction [11], that leverages the temporal correlation between facial expression and speech. A time-domain audio-visual speech separation network, referred to as AV-ConvTasnet in this paper, is another example, which uses pre-trained lip embedding from lip-reading task for speaker extraction [13]. The use of visual cues is intuitively motivated as they are neither corrupted by acoustic noise nor reverberation, furthermore, viseme sequence and phoneme sequence are temporally correlated. However, these methods do not directly use speaker's voice signature as the attractor, which was proven effective in most of the speaker extraction systems.

Visual cues and speaker's voice signature provide complementary information. SpeakerBeam is a technique to leverage both for speaker extraction [14]. But it requires pre-registration of reference speech in advance, which limits the scope of real-world applications. For example, a kiosk or service robot in a public area does not possess pre-registered information of visitors or passers-by. This prompts us to look into speaker extraction scenarios [15] where audio-visual stream of data are available, but speech or face pre-registration of the target speaker is not.

We propose a multi-modal speaker extraction network (MuSE) that uses speech-lip synchronization cue to extract speaker embedding to represents target speaker's voice signature. In this way, neither speaker pre-registration nor reference speech is required. MuSE then uses both speech-lip

*This research is supported by Programmatic Grant No. A18A2b0046 from the Singapore Government's Research, Innovation and Enterprise 2020 plan (Advanced Manufacturing and Engineering domain). It is also supported by Human-Robot Interaction Phase 1 (Grant No. 192 25 00054), the National Research Foundation, Prime Minister's Office, Singapore under the National Robotics Programme.

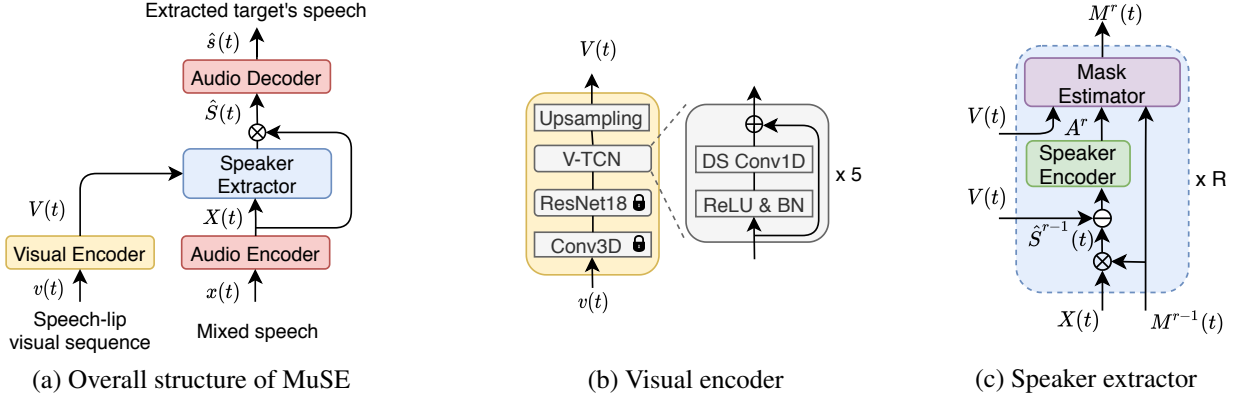


Fig. 1. (a) MuSE is a mask-based structure, consisting of a visual encoder, an audio encoder, a speaker extractor, and a decoder. MuSE seeks to extract a speaker’s voice through masking similar to [13], (b) Visual encoder, (c) The r^{th} extractor block in speaker extractor. \oplus , \otimes refer to point-wise addition and multiplication, \ominus refers to concatenation over temporal dimension.

visual cues and target speaker’s voice signature as the condition to predict target speech. MuSE not only outperforms the baseline in terms of signal and perceptual quality but also shows superior robustness on cross-domain evaluations.

2. MUSE NETWORK

2.1. MuSE vs AV-ConvTasnet

MuSE shares a similar overall network architecture with AV-ConvTasnet, which consist of four parts [13], namely audio encoder, audio decoder, visual encoder, and speaker extractor as shown in Fig. 1(a).

Visual encoder encodes video stream $v(t)$ into a sequence of visual embeddings $V(t)$. Audio encoder transforms the input speech mixture $x(t)$ into latent representation $X(t)$, that is also referred to as speech embedding, while audio decoder renders the extracted speech $\hat{s}(t)$ from its latent representation $\hat{S}(t)$. In AV-ConvTasnet, speaker extractor takes $V(t)$ and $X(t)$ as input, and estimates the mask for target’s speech $M^r(t)$ with $V(t)$ as reference; while in MuSE, speaker extractor performs a similar task, but with a more complex architecture, that is illustrated in Fig. 1(c) and discussed in section 2.4. The MuSE speaker extractor represents the main contributions of this work.

2.2. Audio encoder/decoder

The audio encoder performs 1D convolution on $x(t) \in \mathbb{R}^{1 \times T}$ with a kernel size L and stride $L/2$.

$$X(t) = Conv1D(x(t), L, L/2) \in \mathbb{R}^{N \times K} \quad (1)$$

where N is the speech embedding dimension and $K = (2(T - L))/L + 1$. As $x(t)$ is a time-domain signal, the 1D convolution behaves like a frequency analyzer [5]. The audio decoder performs overlap and add operation to reconstruct

$\hat{s}(t)$ from $\hat{S}(t)$ [16].

$$\hat{s}(t) = Overlap\&Add(\hat{S}(t), L, L/2) \in \mathbb{R}^{1 \times T} \quad (2)$$

$$\hat{S}(t) = X(t) \otimes M_r(t) \in \mathbb{R}^{N \times K} \quad (3)$$

N and L are set to 256 and 40 respectively in this paper.

2.3. Visual encoder

As shown in Fig. 1(b), the visual encoder has a 3D convolutional layer (Conv3D), a ResNet18 block, and a video temporal convolutional block (V-TCN) [13]. The output of V-TCN is up-sampled to match the temporal resolution of speech embedding. The input to the visual encoder are cropped lip images synchronized with speech. Each image is encoded into a single vector embedding of size 512 dimension. Denoted with a lock in the figure, the Conv3D and ResNet18 are pre-trained from lip-reading task first and their weights are fixed during the speaker extraction training. With the visual encoder, we seek to retain the lip-reading ability and encode the viseme movements that synchronizes phoneme sequence of speech.

2.4. Speaker extractor

Speaker extractor is a stack of R extractor blocks, each of which consists of a speaker encoder and a mask estimator. The speaker encoder is designed to produce a target speaker embedding A^r , the mask estimator estimates a mask $M^r(t)$ that only lets pass target speech. A^r is a fixed dimension embedding vector, that encodes an audio-visual sequence of variable length, while $M^r(t)$ is a sequence of masking frames, each corresponds to an input speech frame. They are progressively refined through R repeated blocks. The r^{th} block is shown in Fig. 1(c), with $M^0(t) = X(t)$.

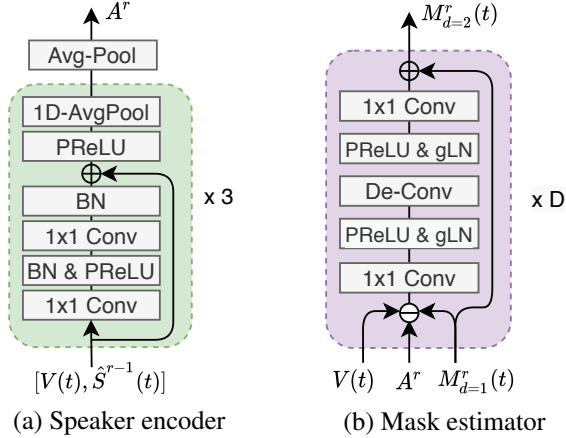


Fig. 2. Architecture and data flow of speaker encoder and mask estimator.

2.4.1. Speaker encoder

As illustrated in Fig. 2(a), speaker encoder consists a stack of three residual blocks followed by an adaptive average pooling layer. The speaker encoder takes a temporal sequence $V(t) \ominus \hat{S}^{r-1}(t)$ as input, where

$$\hat{S}^{r-1} = X(t) \otimes M^{r-1}(t) \quad (4)$$

is the masked speech embedding for target speech from the $(r-1)^{th}$ extractor block. The output is a 256-dimensional single vector A^r , representing the speaker encoded at extractor block r .

2.4.2. Mask estimator

As shown in Fig. 2(b), mask estimator consists of a stack of D audio temporal convolution block (A-TCN) with an exponential growth dilation factor 2^d in the dilated depth-wise separable convolution. The input to the first A-TCN in the stack includes a sequence of visual embeddings $V(t)$, a fixed dimension target speaker embedding A^r , and a sequence of masking frames $M_{d=1}^r(t)$, while to the other A-TCNs are $M_d^r(t)$ only.

2.5. Multi-task learning

To ensure MuSE optimizes both the discriminative speaker embedding and the target speaker’s voice, we propose a multi-task learning framework with two objectives. A scale-invariant signal-to-noise ratio (SI-SDR) [17] loss is to measure the quality between the extracted and clean target speech. The cross-entropy (CE) loss is used for speaker classification. The CE loss is applied to every speaker extractor network in the R repeats of the extractor block. The overall loss is defined in equation 5.

$$\mathcal{L} = \mathcal{L}_{SI-SDR} + \gamma \mathcal{L}_{CE} \quad (5)$$

$$\mathcal{L}_{SI-SDR} = -20 \log_{10} \frac{\|\langle \hat{s}, s \rangle_s\|}{\|\hat{s} - \frac{\langle \hat{s}, s \rangle_s}{\|s\|^2} s\|} \quad (6)$$

$$\mathcal{L}_{CE} = - \sum_{r=1}^R \sum_{c=1}^C y_c^r \log(\text{softmax}(W^r A^r)) \quad (7)$$

where γ is a scaling factor and set to 0.1. s and y are the ground truth target speech and target speaker’s class label respectively. C is the number of speakers in the dataset. W^r is a learnable weight matrix in each output layer for speaker classification.

3. EXPERIMENT SETUP

We develop a MuSE system as described in Section 2, and implement the AV-ConvTasnet as our baseline [13] for comparison. We first evaluate on the VoxCeleb2 dataset [18]. The speakers in the train set and test set do not overlap. All utterances have more than 4 seconds of duration. We obtain 48,000 utterances from 800 speakers in the train set, and 36,237 utterances from 118 speakers in the test set, we create 2 and 3 speakers mixtures of 20,000, 5,000, 3,000 utterances for train, validation and test sets, respectively. Interference speech is mixed with the target speech with a random Signal-to-Noise (SNR) ratio between 10dB to -10 dB. The videos are sampled at 25 FPS. The audio is synchronized with the video and sampled at 16 kHz.

We also compare MuSE and AV-ConvTasnet baseline on cross-domain datasets, namely Grid, TCD-TIMIT, LRS2, LRS3 and AVSpeech datasets [11, 19–22]. Grid and TCD-TIMIT are studio videos while LRS2, LRS3 and AVSpeech are created from BBC, TED videos and YouTube videos, respectively. We generate 3,000 utterances to form a test set for each of the above datasets, following VoxCeleb2 protocol. We notice that the speaking rate in Grid and TCD-TIMIT dataset is lower than others.

The Conv3D and RestNet18 blocks in visual encoder are pre-trained on the LRS2 and LRS3 datasets [21]. In training MuSE, adam optimizer is used with an initial learning rate of $1e^{-3}$. The learning rate is halved if the validation loss increases consecutively for 3 epochs. The training stops when validation loss increases for 5 epochs. The number of extracted blocks R and number of A-TCN blocks D are set to 4 and 8 respectively. During inference, only $\hat{s}(t)$ is extracted while the estimated speaker’s class label in Equation 7 is redundant.

4. EVALUATION RESULTS

4.1. MuSE vs AV-ConvTasnet on VoxCeleb2

We report the performance in terms of SI-SDR (SI-SDR_i) and PESQ [23]. SI-SDR_i measures the speech signal quality while PESQ measures the overall perceptual quality. PESQ is on a scale from 1 to 5, the higher the better. As shown in Table 1, MuSE shows a relative improvement of 10% and 19% in terms of SI-SDR_i over AV-ConvTasnet with 2 speakers and

Table 1. MuSE shows consistent improvement over AV-ConvTasnet on VoxCeleb2 dataset.

Dataset	Model	SI-SDRi (db)	PESQ
2 Spkr	AV-ConvTasnet	10.641	2.065
	MuSE	11.673	2.211
3 Spkr	AV-ConvTasnet	9.778	1.470
	MuSE	11.643	1.623

Table 2. Cross-datasets evaluations (SI-SDR in dB) of the baseline and our model. Models are trained on VoxCeleb2 and tested on other datasets.

Domain	Dataset	Model	2-mix	3-mix
Wild	LRS2	AV-ConvTasnet	10.81	9.50
		MuSE	11.97	11.13
	LRS3	AV-ConvTasnet	12.50	10.52
		MuSE	13.44	12.34
	AVSpeech	AV-ConvTasnet	4.96	2.77
		MuSE	5.88	4.81
Studio	Grid	AV-ConvTasnet	-0.02	-2.81
		MuSE	5.15	1.55
	TCD-TIMIT	AV-ConvTasnet	2.98	1.16
		MuSE	9.86	7.47

3 speakers mixtures. MuSE also has 7% and 10% relative improvement on PESQ.

4.2. MuSE vs AV-ConvTasnet for cross-domain test

We also evaluated MuSE on other audio-visual datasets. As shown in Table 2, we classify the 5 datasets into ‘‘Wild’’ and ‘‘Studio’’ domains. LRS2, LRS3 and AVSpeech belong to ‘‘Wild’’ videos similar to VoxCeleb2. Grid and TCD-TIMIT are collected in studio. On LRS2 and LRS3, AV-ConvTasnet and MuSE perform equally well as they do on VoxCeleb2 dataset. However, their performance both drops on AVSpeech dataset as the visual encoder encounters mismatch data. Nonetheless, MuSE still shows considerable improvement in terms of SI-SDRi over AV-ConvTasnet. When evaluating on out-of-domain datasets, MuSE shows superior robustness to AV-ConvTasnet on both Grid and TCD-TIMIT datasets.

4.3. Comparison with related work

We compare MuSE with recent audio-visual speaker extraction studies on VoxCeleb2 datasets in Table 3 in terms of signal-to-distortion ratio (SDRi). It is observed that MuSE is as competitive as the state-of-the-art method despite that we only used a subset of the VoxCeleb2 dataset for training. We understand that the SDRi results are not directly comparable as they are not trained on exactly the same dataset.

MuSE is different from the ‘Looking to listen at the cocktail party’ [11]. As MuSE uses speech-lip synchronization in-

Table 3. A comparison across various audio-visual speaker extraction implementations on VoxCeleb2 2-speaker mixture, using video (V), a static image (I) or speaker embedding (A) as auxiliary inputs.

Model	Auxiliary input	SDRi (dB)
AVS [24]	V (face) +A	5.9
AV-BLSTM [11, 24]	V (face)	3.25
FaceFilter [25]	I (face)	2.5
AV-U-Net [26]	V (face)	7.6
AV-LSTM [12]	V (lips)	12.1
AV-ConvTasnet	V (lips)	10.9
MuSE	V (lips)	12.0

Table 4. SI-SDRi (dB) of ablation studies on 2-speaker mixture on VoxCeleb2, Grid and TCD-TIMIT datasets. SE refers to speaker embedding.

Model	w/o	VoxCeleb2	Grid	TCD-TIMIT
AV-ConvTasnet	SE	10.64	-0.02	2.98
MuSE-jt	MTL	11.61	0.907	2.27
MuSE	-	11.67	5.15	9.86

formation instead of speech-face synchronization cue, MuSE is expected to generalize well for new speakers.

4.4. Ablation studies

We study a variant of MuSE that is only trained with the SI-SDR loss without the speaker CE loss, referred to as MuSE-jt. As shown in Table 4, MuSE performs similarly with MuSE-jt and AV-ConvTasnet on VoxCeleb2 dataset, but outperforms them in cross-dataset evaluations.

The difference between MuSE and AV-ConvTasnet is the use of speaker embedding. The results validate the benefit of using speaker embedding in MuSE, which represents a more direct speaker reference point than speech-lip synchronization cue alone. The difference between MuSE and MuSE-jt is the use of speaker loss as shown in Equation (7). The results suggest that the speaker loss improves the domain robustness of the system.

5. CONCLUSION

In this paper, we study a new way to extract the speaker embedding by using speech-lip synchronization cue. The visual information and extracted target speaker embedding are used as references to extract the target speaker’s voice. We show that MuSE has a clear advantage over the baseline in both in-domain and out-of-domain tests. We are considering using additional modalities, such as text, as additional input to the mask estimator.

6. REFERENCES

- [1] Adelbert W Bronkhorst, “The cocktail party phenomenon: A review of research on speech intelligibility in multiple-talker conditions,” *Acta Acustica united with Acustica*, vol. 86, no. 1, pp. 117–128, 2000.
- [2] Guoning Hu and DeLiang Wang, “Auditory segmentation based on onset and offset analysis,” *IEEE transactions on audio, speech, and language processing*, vol. 15, no. 2, pp. 396–405, 2007.
- [3] Tuomas Virtanen, “Monaural sound source separation by nonnegative matrix factorization with temporal continuity and sparseness criteria,” *IEEE transactions on audio, speech, and language processing*, vol. 15, no. 3, pp. 1066–1074, 2007.
- [4] John R Hershey, Zhuo Chen, Jonathan Le Roux, and Shinji Watanabe, “Deep clustering: Discriminative embeddings for segmentation and separation,” in *IEEE International Conference on Acoustics, Speech and Signal Processing*. IEEE, 2016, pp. 31–35.
- [5] Yi Luo and Nima Mesgarani, “Conv-TasNet: Surpassing ideal time–frequency magnitude masking for speech separation,” *IEEE/ACM transactions on audio, speech, and language processing*, vol. 27, no. 8, pp. 1256–1266, 2019.
- [6] Chenglin Xu, Wei Rao, Xiong Xiao, Eng Siong Chng, and Haizhou Li, “Single channel speech separation with constrained utterance level permutation invariant training using grid lstm,” in *IEEE International Conference on Acoustics, Speech and Signal Processing*. IEEE, 2018, pp. 6–10.
- [7] Chenglin Xu, Wei Rao, Eng Siong Chng, and Haizhou Li, “SpEx: Multi-scale time domain speaker extraction network,” *IEEE/ACM transactions on audio, speech, and language processing*, 2020.
- [8] Quan Wang, Hannah Muckenhirn, Kevin Wilson, Prashant Sridhar, Zelin Wu, John R Hershey, Rif A Saurous, Ron J Weiss, Ye Jia, and Ignacio Lopez Moreno, “VoiceFilter: Targeted voice separation by speaker-conditioned spectrogram masking,” *Proc. Interspeech*, pp. 2728–2732, 2019.
- [9] Shulin He, Hao Li, and Xueliang Zhang, “Speakerfilter: Deep learning-based target speaker extraction using anchor speech,” in *IEEE International Conference on Acoustics, Speech and Signal Processing*. IEEE, 2020, pp. 376–380.
- [10] Meng Ge, Chenglin Xu, Longbiao Wang, Eng Siong Chng, Jianwu Dang, and Haizhou Li, “SpEx+: A complete time domain speaker extraction network,” in *Proc. Interspeech*, 2020.
- [11] Ariel Ephrat, Inbar Mosseri, Oran Lang, Tali Dekel, Kevin Wilson, Avinatan Hassidim, William T Freeman, and Michael Rubinstein, “Looking to listen at the cocktail party: a speaker-independent audio-visual model for speech separation,” *ACM Transactions on Graphics*, vol. 37, no. 4, pp. 1–11, 2018.
- [12] Triantafyllos Afouras, Joon Son Chung, and Andrew Zisserman, “The Conversation: Deep audio-visual speech enhancement,” *Proc. Interspeech*, pp. 3244–3248, 2018.
- [13] Jian Wu, Yong Xu, Shi-Xiong Zhang, Lian-Wu Chen, Meng Yu, Lei Xie, and Dong Yu, “Time domain audio visual speech separation,” in *IEEE Automatic Speech Recognition and Understanding Workshop*. IEEE, 2019, pp. 667–673.
- [14] Tsubasa Ochiai, Marc Delcroix, Keisuke Kinoshita, Atsunori Ogawa, and Tomohiro Nakatani, “Multimodal speakerbeam: Single channel target speech extraction with audio-visual speaker clues,” *Proc. Interspeech*, pp. 2718–2722, 2019.
- [15] Joseph Roth, Sourish Chaudhuri, Ondrej Klejch, Radhika Marvin, Andrew Gallagher, Liat Kaver, Sharadh Ramaswamy, Arkadiusz Stopczynski, Cordelia Schmid, Zhonghua Xi, et al., “AVA active speaker: An audio-visual dataset for active speaker detection,” in *IEEE International Conference on Acoustics, Speech and Signal Processing*. IEEE, 2020, pp. 4492–4496.
- [16] AV Oppenheim and R Schaffer, “Theory and application of digital signal processing,” *Englewood Cliffs*, 1978.
- [17] Jonathan Le Roux, Scott Wisdom, Hakan Erdogan, and John R Hershey, “SDR–half-baked or well done?,” in *IEEE International Conference on Acoustics, Speech and Signal Processing*. IEEE, 2019, pp. 626–630.
- [18] Joon Son Chung, Arsha Nagrani, and Andrew Zisserman, “VoxCeleb2: Deep speaker recognition,” *Proc. Interspeech*, pp. 1086–1090, 2018.
- [19] Martin Cooke, Jon Barker, Stuart Cunningham, and Xu Shao, “An audio-visual corpus for speech perception and automatic speech recognition,” *The Journal of the Acoustical Society of America*, vol. 120, no. 5, pp. 2421–2424, 2006.
- [20] Naomi Harte and Eoin Gillen, “TCD-TIMIT: An audio-visual corpus of continuous speech,” *IEEE Transactions on Multimedia*, vol. 17, no. 5, pp. 603–615, 2015.
- [21] Triantafyllos Afouras, Joon Son Chung, Andrew Senior, Oriol Vinyals, and Andrew Zisserman, “Deep audio-visual speech recognition,” *IEEE transactions on pattern analysis and machine intelligence*, 2018.
- [22] Triantafyllos Afouras, Joon Son Chung, and Andrew Zisserman, “LRS3-TED: a large-scale dataset for visual speech recognition,” *arXiv preprint arXiv:1809.00496*, 2018.
- [23] Antony W Rix, John G Beerends, Michael P Hollier, and Andries P Hekstra, “Perceptual evaluation of speech quality (PESQ)-a new method for speech quality assessment of telephone networks and codecs,” in *IEEE International Conference on Acoustics, Speech, and Signal Processing. Proceedings*. IEEE, 2001, vol. 2, pp. 749–752.
- [24] Luo Yiyu, Wang Jing, Wang Xinyao, Wen Liang, and Wang Lizhong, “Audio-visual speech separation using i-vectors,” in *IEEE 2nd International Conference on Information Communication and Signal Processing*, 2019, pp. 276–280.
- [25] Soo-Wan Chung, Soyeon Choe, Joon Son Chung, and Hong-Goo Kang, “FaceFilter: Audio-visual speech separation using still images,” *arXiv preprint arXiv:2005.07074*, 2020.
- [26] Andrew Owens and Alexei A Efros, “Audio-visual scene analysis with self-supervised multisensory features,” in *Proceedings of the European Conference on Computer Vision*, 2018, pp. 631–648.